Journal of Organometallic Chemistry 694 (2009) 2270–2278

Contents lists available at ScienceDirect

Journal of Organometallic Chemistry

journal homepage: www.elsevier.com/locate/jorganchem

Dialkyl- and diaryl-platinum(II) complexes with secondary phosphines: Preparation, structure and thermal reaction giving the metallopolymer

Masaki Kakeya, Makoto Tanabe, Yoshiyuki Nakamura, Kohtaro Osakada *

Chemical Resources Laboratory, Tokyo Institute of Technology, 4259 Nagatsuta, Midori-ku, Yokohama 226-8503, Japan

ARTICLE INFO

Article history:
Received 28 January 2009
Received in revised form 4 March 2009
Accepted 6 March 2009
Available online 13 March 2009

Keywords:
Platinum
Secondary phosphine
Thermogravimetry
Metallopolymer

ABSTRACT

Alkyl and arylplatinum complexes with 1,5-cyclooctadiene ligand, [PtR_2(cod)] (R = Me, Ph, C_6H_4-*p*-CF_3, C_6F_5), react with secondary phosphines, PHR'_2 (R′ = *i*-Bu, *t*-Bu, Ph), to afford the mononuclear platinum complexes, *cis*-[$PtR_2(PHR'_2)_2$] (**1a**: R = Me, R′ = *i*-Bu; **1b**: R = Me, R′ = *t*-Bu; **1c**: R = Me, R′ = Ph; **2a**: R = Ph, R′ = *i*-Bu; **2b**: R = Ph, R′ = *t*-Bu; **2c**: R = R′ = Ph; **3a**: R = C_6H_4-*p*-CF_3, R′ = *i*-Bu; **3b**: R = C_6H_4-*p*-CF_3, R′ = *t*-Bu; **3c**: R = C_6H_4-*p*-CF_3, R′ = Ph; **4a**: R = C_6F_5, R′ = *i*-Bu; **4c**: R = C_6F_5, R′ = Ph) in 81–98% yields. Molecular structures of the complexes except for **1a**, **1c** and **2a** were determined by X-ray crystallography. Complex **1b** has a square-planar structure with Pt–C(methyl) bonds of 2.083(8) and 2.109(8) Å, while the Pt–C(aryl) bonds of **2b**–**c**, **3a**–**c**, **4a** and **4c** (2.055(1)–2.073(8) Å) are shorter than them. Thermal decomposition of **1b**, **2a**–**c**, and **3a**–**c** releases methane, biphenyl or 4,4′-bis(trifluoromethyl)biphenyl as the organic products, which are characterized by NMR spectroscopy. The solid product of the thermal reactions of **2b** and **2c** were characterized as the metallopolymers formulated as $[Pt(PR'_2)_2]_n$ (**5b**: R′ = ^{t}Bu; **5c**: R′ = Ph), based on the solid-state NMR and elemental analyses.

1. Introduction

Tertiary phosphines have long been employed as the auxiliary ligands of organotransition–metal complexes and of the transition metal complexes which catalyze the synthetic organic reactions [1–3]. Since the substituents on the phosphorus atom influence the steric and electron-releasing (or -withdrawing) characters of the tertiary phosphines [4], one could obtain the transition metal complexes with desired chemical properties by choosing the phosphines suited as the auxiliary ligands. Dialkyl- and diaryl-complexes of group 10 metals, Ni(II), Pd(II) and Pt(II), with tertiary phosphines ligands, [$MR_2(PR'_3)_2$] (M = Ni, Pd, Pt; R = R′ = alkyl, aryl) were well characterized owing to the rigid square-planar structures as well as to the presence of ^{31}P and/or ^{195}Pt nuclei which render the NMR spectra of the complexes more informative [5–9]. Dialkyl- and diaryl-platinum(II) complexes with tertiary phosphines prefer the *cis*-structure, although dialkylpalladium complexes exist as the *trans*- or *cis*-structure [8,10]. The diarylplatinum complexes undergo thermally induced reductive elimination of the corresponding biaryls [11]. Recent studies on the unsymmetrical diarylplatinum complexes, [Pt(Ar)(Ar′)(dppf)] (DPPF = 1,1′-bis(diphenylphosphino)ferrocene), revealed that the thermodynamic and kinetic parameters for the reductive elimination of biaryl is influenced by the substituents of the aryl ligands [12]. Dialkylplatinum complexes with tertiary phosphine ligands tend to undergo β-hydrogen elimination, giving alkenes, rather than the reductive elimination of alkanes [13].

Secondary phosphines, however, have attracted much less attention than the tertiary phosphines as the auxiliary ligands of the mononuclear organoplatinum complexes. The Pt complexes with the secondary phosphine ligands have recently been reported in relation to the mechanism of hydrophosphination catalyzed by Pd complexes [14]. The secondary phosphines are often reported to lose the P–H hydrogen, upon coordination to Pt to yield the bridging phosphide (PR_2) ligands [15]. The reaction of $PHPh_2$ with a Pt(0) complex affords the cyclic triplatinum complexes with bridging diphenylphosphide ligands probably via oxidative addition of the phosphine ligand to the metal center [16]. Herein, we report the synthesis and molecular structures of the mononuclear platinum complexes with secondary phosphine ligands, *cis*-[$PtR_2(PHR'_2)_2$] (R = Me, Ph, C_6H_4-*p*-CF_3, C_6F_5; R′ = *i*-Bu, *t*-Bu, Ph), as well as their thermal properties.

2. Results and discussion

The reactions of secondary phosphines, PHR'_2 (R′ = *i*-Bu, *t*-Bu, Ph), with [PtR_2(cod)] (R = Me, Ph, C_6H_4-*p*-CF_3, C_6F_5) at room temperature produced the mononuclear platinum complexes formulated as *cis*-[$PtR_2(PHR'_2)_2$] (**1a**: R = Me, R′ = *i*-Bu; **1b**: R = Me, R′ = *t*-Bu; **1c**: R = Me, R′ = Ph; **2a**: R = Ph, R′ = *i*-Bu; **2b**: R = Ph, R′ = *t*-Bu; **2c**: R = R′ = Ph; **3a**: R = C_6H_4-*p*-CF_3, R′ = *i*-Bu; **3b**: R = C_6H_4-*p*-CF_3, R′ = *t*-Bu; **3c**: R = C_6H_4-*p*-CF_3, R′ = Ph; **4a**: R = C_6F_5, R′ = *i*-Bu; **4c**: R = C_6F_5, R′ = Ph), as shown in Scheme 1.

* Corresponding author.
E-mail address: kosakada@res.titech.ac.jp (K. Osakada).

0022-328X/$ - see front matter © 2009 Elsevier B.V. All rights reserved.
doi:10.1016/j.jorganchem.2009.03.009

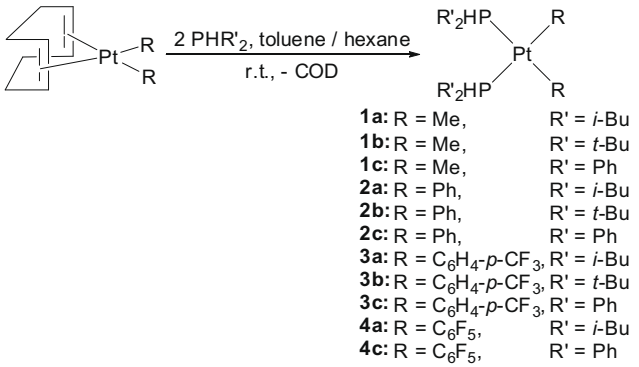

Scheme 1.

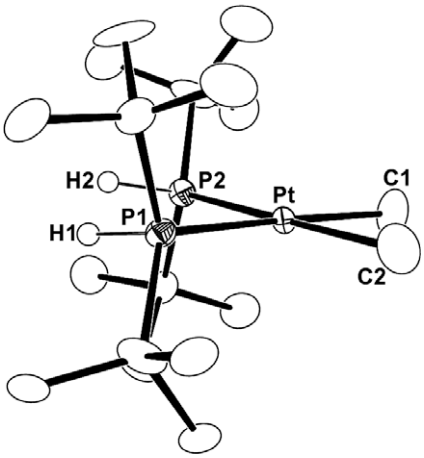

Fig. 1. ORTEP drawing of **1b** with ellipsoids drawn at the 30% probability level. Positions of P–H hydrogens are obtained by calculation. Other hydrogen atoms are omitted in the drawing for simplicity.

Table 1 summarizes the yields and analytical data of the complexes. Complex **4c** was prepared by Forniés et al. and characterized based on the spectroscopic data [17]. A reaction of PH(*t*-Bu)$_2$ with [Pt(C$_6$F$_5$)$_2$(cod)] did not give a phosphine-coordinated complex partly due to the sterically bulky P-ligand and to unfavorable dissociation of the cod owing to a small trans effect of the pentafluorophenyl ligand. Most of the obtained compounds were fully characterized by X-ray crystallography and NMR spectroscopy, while **1a**, **1c** and **2a** were characterized based on the NMR and elemental analyses data.

Figs. 1–4 show the molecular structures of **1b**, **2b**–**c**, **3a**–**c**, **4a** and **4c** determined by X-ray crystallography. Major bond parameters are summarized in Table 2. All these complexes are adopted to square-planar structures around the Pt center, which are coordinated to two secondary phosphine ligands at cis positions and to two methyl or aryl ligands. Pt–C(methyl) bond distances of **1b** are 2.083(8) and 2.109(8) Å, which are longer than Pt–C(aryl) bonds of **2b**–**c**, **3a**–**c**, **4a** and **4c** (2.051(1)–2.077(8) Å) due to significant π-back donation from Pt to the ipso carbon of the aryl ligand.

The molecular structures are classified into three types summarized in Scheme 2, based on conformation of the two secondary phosphine ligands. Complexes **1b** and **3a** contain the two P–H bonds, which are parallel to each other, and orientated toward inner area of the P–Pt–P angle (i). The P–H bonds of **2b**, **3b** and **4c** are also orientated toward the inner area, although they are not parallel (ii). On the other hand, complexes **2c**, **3c** and **4a** have one P–H bond orientated to the inner area of the P–Pt–P, and the other

Table 1
Yields, analytical results, IR data, and melting points of the complexes **1**–**4**.

Complex	Yield (%)[a]	Anal. (%)[b]		IR[c] ν(P–H)	m.p. (°C)
		C	H		
cis-[PtMe$_2$\{PH(*i*-Bu)$_2$\}$_2$] (**1a**)	89	41.69 (41.77)	8.29 (8.57)	2305	–[d]
cis-[PtMe$_2$\{PH(*t*-Bu)$_2$\}$_2$] (**1b**)	94	41.45 (41.77)	8.67 (8.57)	2311 2299	158
cis-[PtMe$_2$(PHPh$_2$)$_2$] (**1c**)	87	52.02 (52.26)	4.75 (4.72)	2330	146
cis-[PtPh$_2$\{PH(*i*-Bu)$_2$\}$_2$] (**2a**)	89	52.15 (52.41)	7.49 (7.54)	2345 2311	168
cis-[PtPh$_2$\{PH(*t*-Bu)$_2$\}$_2$] (**2b**)	95	52.34 (52.41)	7.41 (7.54)	2307	–[e]
cis-[PtPh$_2$(PHPh$_2$)$_2$] (**2c**)	81	60.00 (59.92)	4.33 (4.47)	2341 2328	176
cis-[Pt(C$_6$H$_4$-*p*-CF$_3$)$_2$\{PH(*i*-Bu)$_2$\}$_2$] (**3a**)	91	46.23 (46.33)	6.03 (5.96)	2338	126
cis-[Pt(C$_6$H$_4$-*p*-CF$_3$)$_2$\{PH(*t*-Bu)$_2$\}$_2$] (**3b**)	85	46.21 (46.33)	5.94 (5.96)	2307	160
cis-[Pt(C$_6$H$_4$-*p*-CF$_3$)$_2$(PHPh$_2$)$_2$] (**3c**)	96	52.99 (53.22)	3.50 (3.53)	2336	178
cis-[Pt(C$_6$F$_5$)$_2$\{PH(*i*-Bu)$_2$\}$_2$] (**4a**)	95	41.04 (40.93)	4.54 (4.66)	2363	191
cis-[Pt(C$_6$F$_5$)$_2$(PHPh$_2$)$_2$] (**4c**)[f]	98	–	–	2334	241

[a] Isolated yield.
[b] Calculated values are shown in parentheses.
[c] cm^{-1} in KBr disks.
[d] Oil at room temperature.
[e] Not observed.
[f] Reported by Forniés et al. See Ref. [17].

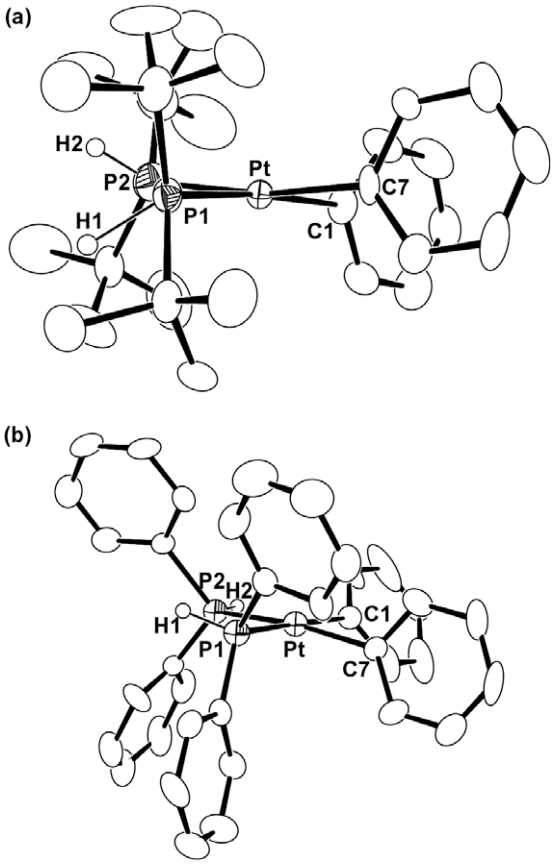

Fig. 2. ORTEP drawings of (a) **2b** and (b) **2c** with ellipsoids drawn at the 30% probability level. One of the two crystallographically independent molecules of **2b** is shown. All the P–H hydrogens of **2b** and one of the P–H hydrogens of **2c** were located by calculation, although position of the remaining P–H hydrogen of **2c** was determined from D-map.

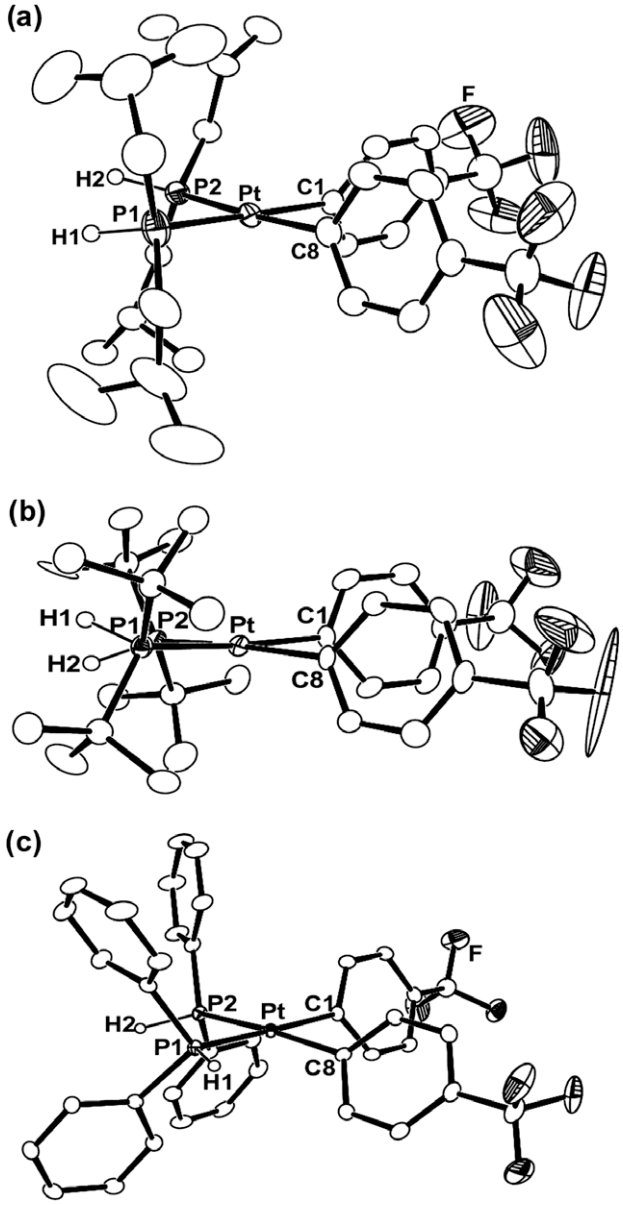

Fig. 3. ORTEP drawings of (a) **3a**, (b) **3b** and (c) **3c** with ellipsoids drawn at the 30% probability level. All the P–H hydrogens were located by calculation, and other hydrogen atoms are omitted in the drawing for simplicity. One of the disordered positions of the fluorine atoms is shown.

P–H bond to the outer area, and these molecules are classified into unsymmetric structure (iii). The complexes with dialkylphosphine ligands except for **4a** belong to (i) or (ii), which the complexes with diphenylphosphine ligands, **2c** and **3c**, prefer the unsymmetrical structure in (iii) the crystalline state.

IR data of the complexes are listed in Table 1. The stretching vibration of the P–H bonds of the secondary phosphine ligands are observed at 2299–2363 cm^{-1}, which are at higher positions than those of the free secondary phosphines ($PH(i\text{-}Bu)_2$: 2284 cm^{-1}, $PH(t\text{-}Bu)_2$: 2278 cm^{-1}, $PHPh_2$: 2286 cm^{-1}). Complexes **1b**, **2a** and **2c** show two peaks for the P–H stretching vibrations. It may be ascribed to the presence of the conformational isomers shown in Scheme 2, although the molecules in the single crystals of each complex were characterized as a single conformational isomer by X-ray crystallography. The shift of P–H stretching vibration of $PH(t\text{-}Bu)_2$ caused by its coordination to the Pt center of **1b**, **2b** and **3b** (21–33 cm^{-1}) is smaller than most of the change of the peak positions of $PH(i\text{-}Bu)_2$ (54–79 Hz) except **1a** (21 Hz) and **2a** (27 Hz for one peak) and of free $PHPh_2$ (42–55 Hz). The ^1H and $^{13}C\{^1H\}$ NMR data of **1**–**4** are listed in Tables 3 and 4, respectively. The two methyl ligands of **1a**–**1c** show the ^1H NMR signals at δ 1.04–1.46 and the $^{13}C\{^1H\}$ NMR signals at δ −0.50 to 5.04. These signals are splitted with reasonable coupling constants, $^2J_{Pt-H}$ = 69–71 Hz and $^1J_{Pt-C}$ = 600–616 Hz. The $^{13}C\{^1H\}$ NMR peaks due to ipso carbons of the aryl ligand of **2**–**4** were observed in the range of δ 145.1–167.6 with J_{Pt-C} = 825–850 Hz. The NMR spectra of the arylplatinum complexes (**2a**–**c**, **3a**–**c**, **4a** and **4c**) exhibit the signals of aromatic hydrogens and carbons, and they are assigned based on the coupling patterns and peak positions. ^1H NMR peaks due to the P–H hydrogen of the complexes with the dialkylphosphine ligands, **1a**–**b**, **2a**–**b**, **3a**–**b** and **4a**, are observed at δ 3.81–4.06, which are at higher magnetic field positions than the free dialkylphosphines ($PH(i\text{-}Bu)_2$: δ 6.76 and $PH(t\text{-}Bu)_2$: δ 5.80). The P–H hydrogen resonances of diphenylphosphine complexes, **1c**, **2c**, **3c** and **4c**, appear in the lower magnetic field region (δ 5.68–5.88) than free $PHPh_2$ (δ 5.19). J_{P-H} values of the complexes with $PH(i\text{-}Bu)_2$ and $PH(t\text{-}Bu)_2$ ligands (**1a**–**b**, **2a**–**b** and **3a**–**b**) (330–350 Hz) are smaller than those of the $PHPh_2$-coordinated complexes **1c**, **2c** and **3c** (360–380 Hz), although the pentafluorophenyl complex with $PH(i\text{-}Bu)_2$ ligands **4a** shows a large J_{P-H} value (360 Hz).

$^{19}F\{^1H\}$ and $^{31}P\{^1H\}$ NMR data of the complexes are listed in Table 5. $^{31}P\{^1H\}$ NMR signals of the ligands, $PH(i\text{-}Bu)_2$ (**1a**, **2a**, **3a** and **4a**), $PH(t\text{-}Bu)_2$ (**1b**, **2b** and **3b**) and $PHPh_2$ (**1c**, **2c**, **3c** and **4c**), are observed at δ −30.2 to −23.0, δ 49.7–59.2 and δ −7.78–3.96,

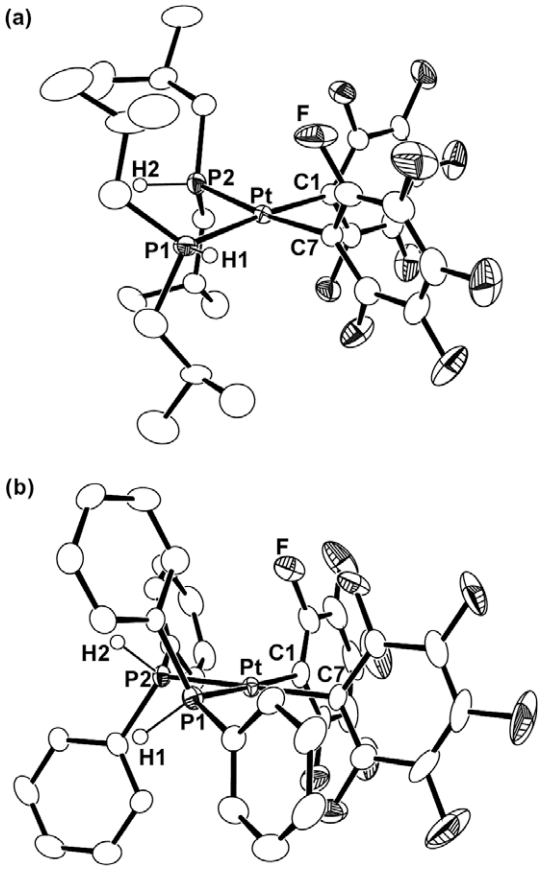

Fig. 4. ORTEP drawings of (a) **4a** and (b) **4c** with ellipsoids drawn at the 30% probability level. All the P–H hydrogens were located by calculation, and other hydrogen atoms are omitted in the drawing for simplicity.

respectively, which are at much lower magnetic field positions than the signals of free secondary phosphines ($PH(i\text{-}Bu)_2$: δ −83.5, $PH(t\text{-}Bu)_2$: δ 20.1, and $PHPh_2$: δ −39.7). The J_{Pt-P} values of the complexes **1a–c**, **2a–c** and **3a–c** are within the range, 1516–1721 Hz, which is similar to those of already reported *cis*-dialkyl- and diphenylplatinum complexes with tertiary phosphine ligands. J_{Pt-P} values of **4a** and **4c** (2304 and 2175 Hz) are larger than the above complexes, indicating a smaller trans influence of the C_6F_5 ligand than the methyl, phenyl, and *p*-(trifluoromethyl)phenyl ligands. The $^{19}F\{^1H\}$ NMR spectra of **4a** and **4c** show signals for the fluorine atoms at ortho position with coupling constants of $^3J_{Pt-F}$ = 318 and 330 Hz, respectively.

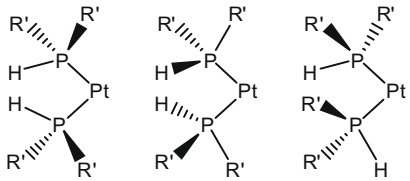

Scheme 2.

Complexes prepared in this study are expected to undergo thermally induced coupling of the methyl and aryl ligands and/or hydrogen loss of the secondary phosphide ligands. Another possible reaction, which may take place upon heating, is the coupling of the methyl (or aryl) ligands with a P–H hydrogen. TG measurement of **1b**, **2b**, **3b** and **4a** was conducted in order to monitor weight loss of the complexes during heating in the solid-state. Fig. 5 compares the thermal weight change of these complexes monitored up to 450 °C. Complexes **1b**, **2b** and **3b** start to decrease the weights at 150 °C, 135 °C, and 160 °C, respectively. The weight loss of **1b** at 200 °C (6%) corresponds to that calculated by assuming evolution of methane (see below) from the starting molecule. Complexes **2b** and **3b** undergo initial decrease of the weight below 190 °C, and the weight loss at that temperature (24% and 38%) corresponds to those calculated assuming reductive elimination of biphenyl from **2b** (24%) and of 4,4′-bis(trifluoromethyl)biphenyl from **3b** (37%), respectively. Complex **4a** is thermally more stable, and starts thermal weight decrease above 180 °C. Weight loss at 270–330 °C (65%) is larger than that obtained by assuming elimination of two pentafluorophenyl ligands, and it can be ascribed to the decomposition including elimination of the phosphine ligands. Complexes **1b**, **2b** and **3b** also show further thermal decomposition at 260–330 °C. These results suggest that complexes **1b**, **2b** and **3b** undergo elimination of methane or reductive elimination of biaryls at the initial stage of thermolysis and that thermolysis of **4a** with the more stable Pt–C bonds occurs at much higher temperature, and accompanies elimination of the phosphine ligands.

Table 2
Selected bond lengths (Å) and bond angles (°) for **1b**, **2b–c**, **3a–c**, **4a** and **4c**.

	1b	2b[a]	2c	3a	3b	3c	4a	4c
Bond lengths (Å)								
Pt–C1	2.083(8)	2.065(7)	2.065(7)	2.054(3)	2.070(6)	2.051(3)	2.067(4)	2.070(3)
Pt2–C29		2.065(8)						
Pt–C2, C7, C8[b]	2.109(8)	2.072(7)	2.071(8)	2.068(3)	2.061(6)	2.057(3)	2.073(5)	2.067(3)
Pt2–C35		2.077(8)						
Pt–P1	2.306(2)	2.319(2)	2.288(2)	2.296(1)	2.340(2)	2.300(1)	2.276(1)	2.277(1)
Pt2–P3		2.338(2)						
Pt–P2	2.288(2)	2.343(2)	2.283(2)	2.301(1)	2.343(2)	2.275(1)	2.276(2)	2.286(1)
Pt2–P4		2.343(2)						
Bond angles (°)								
P1–Pt–P2	92.33(7)	90.67(8)	95.40(6)	95.88(3)	92.28(6)	93.9(1)	94.27(5)	90.41(3)
P3–Pt2–P4		91.l3(7)						
P2–Pt–C1	93.4(2)	96.2(2)	89.2(2)	88.3(1)	93.5(2)	90.2(1)	89.2(2)	90.7(1)
P4–Pt2–C29		94.7(2)						
C1–Pt–C2, C7, C8[b]	82.2(3)	81.9(3)	86.7(3)	87.1(1)	80.1(2)	87.5(2)	88.6(2)	88.1(1)
C29–Pt2–C35		82.0(3)						
P1–Pt–C2, C7, C8[b]	92.1(2)	92.0(2)	88.8(2)	88.7(1)	94.5(2)	88.6(1)	88.3(1)	90.8(1)
P3–Pt2–C35		92.2(2)						

[a] Parameters of two crystallographically independent molecules are shown.
[b] C2 for **1b**; C7 for **2b**, **2c**, **4a** and **4c**; C8 for **3a–c**.

Table 3
^{1}H NMR spectroscopic data for **1–4**.[a]

	PtR	PH	PR′$_2$H
1a	1.04 (dd, CH_3, 6H, $^3J_{P-H}$ = 7.2, 9.0 Hz, J_{Pt-H} = 69 Hz)	4.06(m, 2H, J_{P-H} = 330 Hz, $^3J_{P-H}$ = 7.3 Hz)	1.91 (septet, C*H*, 4H), 1.63 (m, CH_2, 8H) 0.94 (d, CH_3, 12H, $^3J_{H-H}$ = 6.6 Hz) 0.87 (d, CH_3, 12H, $^3J_{H-H}$ = 6.6 Hz)
1b	1.23 (apparent triplet, CH_3, 6H, $^3J_{P-H}$ = 6.4 Hz, $^2J_{Pt-H}$ = 70 Hz)	3.67 (brm, 2H, J_{P-H} = 330 Hz, $^3J_{P-H}$ = 13 Hz)	1.29 (s, 9H, CH_3) 1.26 (s, 9H, CH_3)
1c	1.46 (dd, CH_3, $^2J_{P-H}$ = 6.9, 9.9 Hz, J_{Pt-H} = 71 Hz)	5.82 (brm, 2H, J_{P-H} = 360 Hz, $^3J_{P-H}$ = 10 Hz)	7.40 (m, 8H, *ortho*) 6.94 (m, 12*H*, *para* and *meta*)
2a	7.70 (tt, 4H, *ortho*, J_{Pt-H} = 59 Hz, $^3J_{H-H}$ = 6.0 Hz) 7.18 (t, 4H, *meta*, $^3J_{H-H}$ = 6.0 Hz) 6.92 (t, 2H, *para*, $^3J_{H-H}$ = 6.0 Hz)	3.99 (m, 2H, J_{P-H} = 330 Hz, $^3J_{P-H}$ = 6.3 Hz)	1.98 (m, 4H, C*H*), 1.47 (m, 4H, CH_2) 1.29 (m, 4H, CH_2) 0.97 (d, 6H, CH_3, $^3J_{H-H}$ = 6.6 Hz) 0.83 (d, 6H, CH_3, $^3J_{H-H}$ = 6.6 Hz)
2b	7.77 (t, 4H, *ortho*, $^3J_{H-H}$ = 6.3 Hz, $^3J_{Pt-H}$ = 31 Hz) 7.08 (t, 4H, *meta*, $^3J_{H-H}$ = 7.8 Hz) 6.92 (t, 2H, *para*, $^3J_{H-H}$ = 6.9 Hz)	3.83 (m, 2H, J_{P-H} = 330 Hz, $^3J_{P-H}$ = 19 Hz)	1.21 (s, 9H, CH_3) 1.17 (s, 9H, CH_3)
2c	7.73 (t, 4H, *ortho*, $^3J_{H-H}$ = 6.3 Hz, J_{Pt-H} = 62 Hz) 7.08 (t, 4H, *meta*, $^3J_{H-H}$ = 6.0 Hz), 6.92 (m, 2H, *para*)	5.88 (m, 2H, P*H*, J_{P-H} = 370 Hz)	7.27 (t, 8*H*, *ortho*, $^3J_{H-H}$ = 7.8 Hz) 6.92 (m, 12H, *meta*, *para*)
3a	7.57 (tt, 4H, *ortho*, $^3J_{H-H}$ = 5.7 Hz, $^3J_{Pt-H}$ = 23 Hz) 7.40 (t, 4H, *meta*, $^3J_{H-H}$ = 6.9 Hz)	3.85 (m, 2H, P*H*, J_{P-H} = 330 Hz, $^3J_{P-H}$ = 6.6 Hz)	1.84 (m, 4H, C*H*), 1.24 (m, 8H, CH_2) 0.89 (d, 12H, CH_3, $^3J_{H-H}$ = 6.6 Hz) 0.76 (d, 12H, CH_3, $^3J_{H-H}$ = 6.6 Hz)
3b	7.54 (tt, 4H, *ortho*, $^3J_{H-H}$ = 6.0 Hz, $^3J_{Pt-H}$ = 59 Hz) 7.02 (d, 4H, *meta*, $^3J_{H-H}$ = 7.8 Hz)	3.81 (m, 2H, P*H*, J_{P-H} = 350 Hz, $^3J_{P-H}$ = 18 Hz)	1.06 (s, 9H, CH_3) 1.02 (s, 9H, CH_3)
3c	7.54 (tt, 4H, *ortho*, J_{H-H} = 6.9 Hz, J_{Pt-H} = 30 Hz) 7.02 (t, 4H, *meta*, J_{H-H} = 7.2 Hz)	5.68 (br-m, 2H, P*H*, J_{P-H} = 380 Hz, $^3J_{P-H}$ = 6.6 Hz)	7.11 (m, 8H, *para*) 6.91 (m, 12*H*, *ortho*, *meta*)
4a		4.00 (m, 2H, P*H*, J_{P-H} = 360 Hz, $^3J_{P-H}$ = 7.2 Hz)	1.89 (m, 4H, C*H*), 1.39 (m, 8H, CH_2) 0.86 (d, 12H, CH_3, $^3J_{H-H}$ = 6.6 Hz) 0.74 (d, 12H, CH_3, $^3J_{H-H}$ = 6.6 Hz)
4c	Ref. [17]	Ref. [17]	Ref. [17]

[a] At 300 MHz in C_6D_6 at room temperature except for **1b**. At 400 MHz in C_6D_6 at room temperature for **1b**.

Table 4
^{13}C{^{1}H} NMR spectroscopic data for **1–4**.[a]

	PtR	PR′$_2$H
1a	1.69 (dd, CH_3, $^2J_{Ptrans-C}$ = 9 Hz, $^2J_{Pcis-C}$ = 10 Hz, J_{Pt-C} = 601 Hz)	31.3 (d, CH_2, J_{P-C} = 3 Hz, $^2J_{Pt-C}$ = 15 Hz), 26.6 (apparent triplet, C*H*, $^2J_{P-C}$ = 9 Hz), 24.4 (apparent triplet, CH_3, $^3J_{P-C}$ = 5 Hz), 23.6 (apparent triplet, CH_3, $^3J_{P-C}$ = 3 Hz)
1b	−0.50 (dd, CH_3, $^2J_{Ptrans-C}$ = 11 Hz, $^2J_{Pcis-C}$ = 100 Hz, J_{Pt-C} = 600 Hz)	33.8 (m, CCH_3), 32.1 (d, CCH_3, $^2J_{P-C}$ = 4 Hz, $^3J_{Pt-C}$ = 11 Hz)
1c	5.04 (dd, CH_3, $^2J_{Ptrans-C}$ = 8 Hz, $^2J_{Pcis-C}$ = 101 Hz, J_{Pt-C} = 616 Hz)	134.1 (apparent triplet, *ortho*, $^2J_{P-C}$ = 5 Hz), 130.7 (m, *ipso*), 129.9 (s, *para*), 128.4 (apparent triplet, *meta*, $^3J_{P-C}$ = 5 Hz)
2a	161.3 (dd, *ipso*, $^2J_{Ptrans-C}$ = 114 Hz, $^2J_{Pcis-C}$ = 13 Hz, J_{Pt-C} = 840 Hz), 137.0 (t, *meta*, $^3J_{Pt-C}$ = 17 Hz), 127.8 (t, *ortho*, $^2J_{Pt-C}$ = 2 Hz), 122.2 (t, *para*, $^4J_{Pt-C}$ = 6 Hz)	30.2 (m, C*H*, $^2J_{P-C}$ = 31 Hz), 26.7 (t, CH_2, J_{P-C} = 8 Hz), 24.4 (t, CH_3, $^3J_{P-C}$ = 5 Hz), 23.5 (t, CH_3, $^3J_{P-C}$ = 5 Hz)
2b	157.6 (dd, *ipso*, $^2J_{Ptrans-C}$ = 110 Hz, $^2J_{Pcis-C}$ = 12 Hz, J_{Pt-C} = 843 Hz), 138.7 (t, *ortho*, $^2J_{Pt-C}$ = 18 Hz), 127.2 (t, *para*, $^4J_{Pt-C}$ = 2 Hz), 121.7 (t, *meta*, $^3J_{Pt-C}$ = 6 Hz)	34.6 (m, CCH_3, J_{P-C} = 20 Hz), 32.2 (s, CCH_3)
2c	160.3 (dd, *ipso*, $^2J_{Ptrans-C}$ = 113 Hz, $^2J_{Pcis-C}$ = 13 Hz, J_{Pt-C} = 850 Hz), 128.5 (m, *ortho* overlapped with C_6D_6), 122.6 (t, *meta*, $^3J_{Pt-C}$ = 43 Hz)	137.4 (t, *meta*, $^3J_{Pt-C}$ = 15 Hz), 134.1 (apparent triplet, *ortho*, $^2J_{P-C}$ = 6 Hz), 130.2 (s, *para*), 129.5 (s, *ipso*)
3a	167.6 (m, *ipso*, $^2J_{Ptrans-C}$ = 112 Hz, $^2J_{Pcis-C}$ = 13 Hz, J_{Pt-C} = 840 Hz), 140.0 (brt, *para*), 136.8 (t, *meta*, $^3J_{Pt-C}$ = 36 Hz), 123.8 (m, *ortho*), 126.1 (quartet, CF_3, J_{F-C} = 271 Hz)	30.2 (m, C*H*), 26.6 (apparent triplet, CH_2, J_{P-C} = 8 Hz), 24.3 (apparent triplet, CH_3, $^2J_{P-C}$ = 5 Hz), 23.4 (apparent triplet, CH_3, $^2J_{P-C}$ = 5 Hz)
3b	164.0 (dd, *ipso*, $^2J_{Ptrans-C}$ = 108 Hz, $^2J_{Pcis-C}$ = 12 Hz), 136.1 (brm, *para*), 125.3 (d, CF_3, J_{F-C} = 229 Hz), 123.1 (t, *ortho*, $^2J_{Pt-C}$ = 67 Hz)	34.6 (m, CCH_3, J_{P-C} = 10 Hz), 31.9 (s, CCH_3, $^2J_{P-C}$ = 218 Hz, $^3J_{Pt-C}$ = 422 Hz)
3c	166.0 (m, *ipso*, $^2J_{Ptrans-C}$ = 112 Hz, $^2J_{Pcis-C}$ = 11 Hz, J_{Pt-C} = 825 Hz), 137.0 (t, *meta*, $^3J_{Pt-C}$ = 18 Hz), 129.3 (s, *para*), 125.3 (quartet, CF_3, J_{F-C} = 270 Hz), 123.9 (t, *ortho*, $^2J_{P-C}$ = 34 Hz)	137.8 (s, *ipso*), 133.8 (m, *ortho*), 130.6 (s, *para*), 128.7 (m, *meta*)
4a	146.9 (dd, *ortho*, J_{F-C} = 229 Hz, $^2J_{Pt-C}$ = 18 Hz), 137.9 (m, *meta* and *para*, J_{F-C} = 248 Hz)	31.4 (d, CH_2, J_{P-C} = 10 Hz, $^2J_{Pt-C}$ = 34 Hz), 26.3 (apparent triplet, C*H*, $^2J_{P-C}$ = 9 Hz), 24.1 (apparent triplet, CH_3, $^3J_{P-C}$ = 6 Hz), 23.1 (apparent triplet, CH_3, $^3J_{P-C}$ = 2 Hz)
4c	148.3 (m, *ortho*), 145.1 (m, *ipso*), 139.7 (m, *para*), 136.3 (m, *meta*)	133.5 (m, *ortho*),131.2 (s, *para*), 128.7 (m, *meta*), 125.4 (apparent triplet, *ipso*, $^3J_{P-C}$ = 38 Hz)

[a] At 75 MHz in C_6D_6 at room temperature except for **1b**. At 100 MHz in C_6D_6 at room temperature for **1b**.

Heating complexes **1a–c** in a pressure-resistant NMR tube at 150 °C for 18 h in C_6D_6/*n*-$C_{11}H_{24}$ (3:1) forms CH_4 which is characterized by ^{1}H NMR spectra of the reaction mixtures. Thermal reactions of **2a–c** and **3a–c** in undecane at 180 °C (18 h) and ^{1}H NMR measurement of a part of the reaction mixture in $CDCl_3$ showed formation of biphenyl and 4,4′-bis(trifluoromethyl)biphenyl, respectively. Products of thermolysis of **4a** and **4c** formed by TG measurement up to 330 °C, however, did not contain decafluorobiphenyl.

Pt-containing products of the thermal reactions of **2b** and **2c** (200 °C for 18 h) are obtained as yellow solids after washing the

Table 5
$^{31}P\{^1H\}$ and $^{19}F\{^1H\}$ NMR spectroscopic data for **1**–**4**.

	$^{31}P\{^1H\}$[a]	$^{19}F\{^1H\}$[b]
1a	−23.0 (J_{Pt-P} = 1721 Hz)	
1b	59.2 (J_{Pt-P} = 1705 Hz)	
1c	3.96 (J_{Pt-P} = 1721 Hz)	
2a	−29.3 (J_{Pt-P} = 1624 Hz)	
2b	51.0 (J_{Pt-P} = 1574 Hz)	
2c	0.75 (J_{Pt-P} = 1516 Hz)	
3a	−30.2 (J_{Pt-P} = 1673 Hz)	−61.9 (s, CF_3)
3b	49.7 (J_{Pt-P} = 1630 Hz)	−61.9 (s, CF_3)
3c	−1.47 (J_{Pt-P} = 1663 Hz)	−59.9 (s, CF_3)
4a	−29.6 (J_{Pt-P} = 2304 Hz)	−115.0 (apparent triplet, C_6F_5 *ortho*, $^3J_{Pt-F}$ = 318 Hz, $^4J_{P-F}$ = 160 Hz), −158.6 (s, C_6F_5 *para*), −160.9 (s, C_6F_5 *meta*)
4c	−7.78 (J_{Pt-P} = 2175 Hz)	Ref. [17]

[a] At 121 MHz in C_6D_6 at room temperature.
[b] At 376 MHz in C_6D_6 at room temperature.

product with hexane. The following data of the product indicate formation of the Pt-containing polymers, **5b** and **5c**, as shown in Scheme 3.

The IR spectra of **5b** and **5c** do not show a peak assignable to the P–H bond stretching vibration. The results of elemental analysis are consistent with the value calculated as the doubly phosphide-bridged platinum complexes. Fig. 6 shows the solid-state CPMAS $^{31}P\{^1H\}$ NMR spectrum of **5b**, which shows a single signal at δ 73.4 franked with ^{195}Pt nucleus (J_{Pt-P} = 1770 Hz). The peak position as well as that of **5c** (δ 81.3, J_{Pt-P} = 2130 Hz) are shifted to lower magnetic field positions compared with that of the mononuclear platinum complexes **2b** (δ 51.0) and **2c** (δ 0.75) in the solution. The J_{Pt-P} values change, depending on the bridging ligands. Glueck reported that cationic Pt(II) complexes with doubly bridging phosphide ligands, $[\{Pt(dppe)\}_2(\mu\text{-PRMes})_2][BF_4]_2$ (R = H, Me; Mes = 2,4,6-$C_6H_2Me_3$) and $[\{Pt(dppe)\}_2(\mu\text{-PMeMes})(\mu\text{-PMes})][BF_4]$ showed J_{Pt-P} values in the range, 1632–1770 and 1898 Hz, respectively [19]. On the other hand J_{Pt-P} value of neutral Pt(II) complexes with bridging phosphinidene ligands (μ-PMes), $[\{Pt(dppe)\}_2(\mu\text{-PMes})_2]$ and $[\{Pt(dppe)\}_2(\mu\text{-PMeMes})(\mu\text{-PMes})][BF_4]$ showed J_{Pt-P} values, 805 and 744 Hz, respectively [19]. Leoni reported that a neutral Pt(I) complex with doubly μ-P(*t*-Bu)$_2$ ligands and a Pt–Pt bond, $[\{PtL\{PH(t\text{-}Bu)_2\}\{\mu\text{-}P(t\text{-}Bu)_2\}_2]$ (L = CO, PH(*t*-Bu)$_2$) show J_{Pt-P} value of 2431–2670 Hz, and Mastrorilli reported a neutral Pt(II) complex without Pt–Pt bond [20], $[\{PtH_2\{PH(t\text{-}Bu)_2\}_2\{\mu\text{-}P(t\text{-}Bu)_2\}_2]$ shows J_{Pt-P} value of 1963 Hz [21]. Although J_{Pt-P} value of **5b** are higher than those, which is closer to a neutral Pt(II) complex without Pt–Pt bond than that of a Pt–Pt bond. Forniés reported that a cationic trinuclear Pt(II) complex with μ-PPh_2 ligands, $[Pt_3(C_6F_5)_3\{PPh_2(C_6F_5)\}(\mu\text{-}PPh_2)_3]$ shows J_{Pt-P} value in the range, 1964–2263 Hz. The J_{Pt-P} value of **5c** is in the range of these values [22]. The cyclic complex with the bridging phosphide group without Pt(I)–Pt(II) bond, $[Pt_3H(\mu\text{-}PPh_2)_3(PEt_3)_3]$ (1960, 2239 Hz) show large Pt–P coupling constants [16]. Thus, **5b** and **5c** are proposed to have the multinuclear structure with the bridging phosphide ligands, as shown in Scheme 3, although the solid-state NMR data did not provide useful information to determine the more detailed structures.

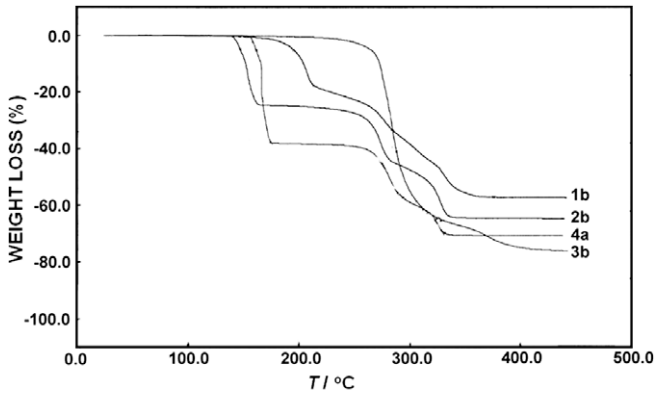

Fig. 5. Thermogravimetric curves of (a) **1b**, (b) **2b**, (c) **3b** and (d) **4a**. Measurements were performed under a stream of nitrogen. Rate of the temperature was 10 °C min^{-1} during the measurements.

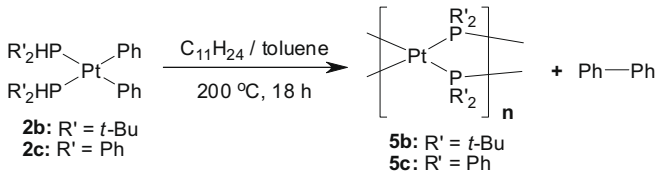

Scheme 3.

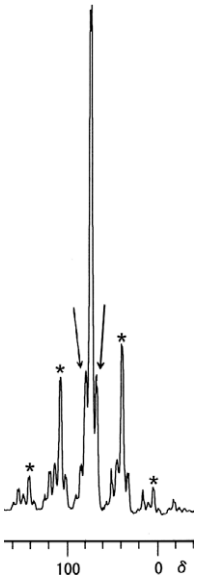

Fig. 6. CPMAS $^{31}P\{^1H\}$ NMR spectrum of **5b**. Signals marked with arrows are assigned to ^{195}Pt satellite signals. The satellites due to the ^{195}Pt–^{31}P–^{195}Pt isotopomer are not observed probably due to low intensity. Signals with asterisk are due to the spinning side band that resulted from the spinning speed of 5 kHz.

3. Conclusion

We demonstrated the preparation and structure of the methyl- and arylplatinum complexes having two secondary phosphine ligands are the presence of conformational isomers of the ligands in the crystal state. Thermal degradation of the complexes causes elimination of methane or coupling of two aryl ligands depending on the kind of the ligands. The thermal reaction of **2b** and **2c** yields multinuclear complexes with bridged phosphide ligands as the solid products.

4. Experimental

4.1. General remark

All manipulations of the complexes were carried out using standard Schlenk techniques under an argon or nitrogen atmosphere. Hexane and toluene were purified by passing through a solvent purification system (Glass Contour). ^1H, $^{13}C\{^1H\}$, $^{19}F\{^1H\}$, and

Table 6
Crystallographic data and details of refinement for **1b**, **2b–c**, **3a–c**, **4a** and **4c**.

	1b	**2b**	**2c**	**3a**	**3b**	**3c**	**4a**	**4c**
Formula	$C_{18}H_{44}P_2Pt$	$C_{56}H_{85}P_2Pt$	$C_{36}H_{32}P_2Pt$	$C_{30}H_{46}F_6P_2Pt$	$C_{30}H_{46}F_6P_2Pt$	$C_{38}H_{30}F_6P_2Pt{\cdot}C_7H_8$	$C_{28}H_{38}F_{10}P_2Pt$	$C_{36}H_{22}F_{10}P_2Pt$
Formula weight	517.56	1272.36	721.65	777.72	777.72	949.82	821.63	901.59
Crystal system	Orthorhombic	Monoclinic	Orthorhombic	Monoclinic	Triclinic	Monoclinic	Monoclinic	Orthorhombic
Space group	$Pna2_1$ (No. 33)	$P2_1/n$ (No. 14)	$Pnma$ (No. 62)	$P2_1/n$ (No. 14)	$P\bar{1}$ (No. 2)	$P2_1/a$ (No. 14)	$P2_1/n$ (No. 14)	$P2_12_12_1$ (No. 19)
Crystal size (mm)	0.40 × 0.30 × 0.18	0.12 × 0.10 × 0.10	0.12 × 0.10 × 0.04	0.25 × 0.13 × 0.10	0.23 × 0.21 × 0.15	0.33 × 0.20 × 0.10	0.25 × 0.20 × 0.08	0.20 × 0.15 × 0.10
Crystal color	Colorless	Colorless	Colorless	Colorless	Colorless	Colorless	Colorless	Colorless
a (Å)	14.086(5)	16.690(5)	19.714(2)	14.625(3)	11.382(6)	14.098(2)	10.105(2)	12.560(2)
b (Å)	8.569(3)	21.020(6)	16.306(2)	13.582(3)	11.649(6)	18.657(2)	15.331(3)	14.681(3)
c (Å)	18.696(7)	17.860(6)	9.303(1)	17.408(4)	13.417(7)	15.242(2)	21.242(5)	17.892(3)
α (°)					86.42(2)			
β (°)		112.970(4)		103.8770(9)	68.37(2)	99.712(2)	100.785(1)	
γ (°)					88.32(2)			
V (Å^3)	2257(2)	5769(3)	2990.5(6)	3357(1)	1650(2)	3951(1)	3232.7(1)	3299(1)
Z	4	4	4	4	2	4	4	4
Dcalc (g cm^{-3})	1.523	1.465	1.603	1.539	1.565	1.596	1.688	1.815
F(000)	1040	2548	1424	1552	776	1880	1616	1744
μ (mm^{-1})	6.355	4.969	4.804	4.309	4.382	3.677	4.497	4.416
Number of reflections measured	15672	42278	21932	23631	11396	28854	21267	24354
Number of unique reflections	2627	13182	3531	7381	6882	9003	6930	7481
Rint	0.0440	0.058	0.056	0.022	0.034	0.036	0.037	0.026
Number of observed reflections ($I > 2\sigma(I)$)	2154	9935	2834	6236	5569	7659	5413	6282
Number of variables	204	651	341	450	404	471	414	462
R_1 ($I > 2\sigma(I)$)	0.0524	0.0622	0.0331	0.0309	0.0403	0.326	0.0379	0.0203
wR_2 ($I > 2\sigma(I)$)	0.1361	0.1547	0.0777	0.0810	0.0996	0.0920	0.0841	0.0288
Goodness-of-fit (GOF)	1.090	1.002	1.157	0.997	1.009	0.969	1.018	0.836

$^{31}P\{^{1}H\}$ NMR spectra were recorded on Varian Mercury 300 and JEOL EX-400 spectrometers. The peak positions of the $^{19}F\{^{1}H\}$ and $^{31}P\{^{1}H\}$ NMR spectra were referenced to an external CF_3COOH (δ −74.1) and to an external 85% H_3PO_4, respectively. Solid-state CPMAS $^{31}P\{^{1}H\}$ NMR measurement was carried out at 161.7 MHz on a JEOL ECA-400 spectrometer using spinning speed of 5330 Hz. ^{31}P chemical shift was referenced to $(NH_4)_2HPO_4$ (δ 1.60). [PtR_2(cod)] (R = Me [18a], Ph [18b], C_6H_4-*p*-CF_3 [18c], C_6F_5 [5b]) was prepared according to the reported procedure. A secondary phosphines, PHR'_2 (R′ = *i*-Bu, *t*-Bu, Ph), and *n*-undecane (*n*-$C_{11}H_{24}$) are commercially available products from Strem Chemicals and Wako Pure Chemical Industries. These employed in the research were in the reagent grade and used as received without further purification. IR absorption spectra were recorded on a Shimadzu FT/IR-8100 spectrometer. Elemental analysis was carried out with a LECO CHNS-932 or Yanaco MT-5 CHN autorecorder. Thermogravimetric analysis (TGA) experiments were conducted using a Seiko Instruments Inc. TG/DTA 6200R. Dry samples were weighted (10–20 mg) into a platinum pan and were heated at 10 °C min^{-1} under a stream of N_2.

4.2. Synthesis of cis-[$PtMe_2(PR_2H)_2$] (**1a**: R = i-Bu, **1b**: t-Bu, **1c**: Ph)

Secondary phosphines, PR_2H (R = ^{i}Bu: 0.10 mL, ^{t}Bu: 0.12 mL, Ph: 0.12 mL; 0.66 mmol), were added to a *n*-hexane solution (3 mL) of [$PtMe_2$(cod)] (100 mg, 0.30 mmol) and the reaction mixture was stirred for 3 h at room temperature. The solution of **1a** was filtered to remove by-products, the resultant filtrate was concentrated under reduced pressure to obtain complex **1a** as a colorless oil (123 mg). The crude solids, which were precipitated from the reaction mixture of **1b** and **1c**, were washed with hexane (3 mL × 3) and dried in vacuo. Crystals of **1b** suitable for X-ray crystallography were obtained by recrystallization from toluene/*n*-hexane (**1b**, 1 mL/4 mL; **1c**, 8 mL/1 mL) at room temperature (**1b**, 146 mg; **1c**, 116 mg).

4.3. Synthesis of cis-[$PtR_2(PR'_2H)_2$] (R = Ph, **2a**: R′ = i-Bu, **2b**: t-Bu, **2c**: Ph; R = C_6H_4-p-CF_3, **3a**: R′ = i-Bu, **3b**: t-Bu, **3c**: Ph; R = C_6F_5, **4a**: R′ = i-Bu, **4c**: Ph)

Secondary phosphines, PR_2H (R = *i*-Bu: 0.21 mL), were added to a toluene/*n*-hexane solution (3 mL/2 mL) of [$PtPh_2$(cod)] (300 mg, 0.66 mmol) and the reaction mixture was stirred for 1 h at room temperature. The crude solids, which were precipitated from the reaction mixture of **2a**, were washed with hexane (3 mL × 3) and dried in vacuo. Crystal of **2a** was obtained by recrystallization from toluene/*n*-hexane (**2a**, 6 mL/1 mL) at room temperature to give a colorless crystal (**2a**, 376 mg). Complexes **2b**–**c**, **3a**–**c**, **4a** and **4c** were synthesized in a similar manner to 4.1. The crude solids, which were precipitated from the reaction mixtures from **2a**–**c**, **3a**–**c**, **4a** and **4c**, were washed with hexane (3 mL × 3) and dried in vacuo. Crystals of **2b**, **2c**, **3a**–**c**, **4a** and **4c** suitable for X-ray crystallography were obtained by recrystallization from toluene/*n*-hexane.

4.4. Thermal reactions of **2b** and **2c**

Heating reactions of toluene/*n*-undecane (2 mL/2 mL) solutions of **2b** (1.0 g, 1.56 mmol) and of **2c** (500 mg, 0.69 mmol) at 200 °C caused a precipitation from the reaction mixture, respectively. The mixture was filtered to collect the precipitates and the obtained solid was washed with 10 mL of *n*-hexane and dried in vacuo to yield yellow solid products (**5b**, 370 mg, 49%; **5c**, 270 mg, 69%). The filtrate and washings of the reaction of **2c** were dried in vacuo and the formed biphenyl (85.4 mg, 80%). Data for **5b**: solid-state CPMAS $^{31}P\{^{1}H\}$ NMR (161 MHz, r.t.): δ 73.4 (J_{Pt-P} = 1770 Hz). Anal. Calc. for $C_{16}H_{36}P_2Pt$: C, 39.58; H, 7.47. Found: C, 39.36; H, 7.88%. Data for **5c**: solid-state CPMAS $^{31}P\{^{1}H\}$ NMR (161 MHz, r.t.): δ 81.3 (J_{Pt-P} = 2130 Hz). Anal. Calc. for $C_{24}H_{20}P_2Pt$: C, 50.98; H, 3.57. Found: C, 50.67; H, 3.70%.

4.5. X-ray crystallography

Crystals of **1b**, **2b**–**c**, **3a**–**c**, **4a** and **4c** suitable for X-ray diffraction study were mounted in glass capillaries. All of data were collected at −160 °C on a Rigaku Saturn CCD diffractometer equipped with monochromated Mo Kα radiation (λ = 0.71073 Å). Crystal Structure, version 3.8 for Windows. A full-matrix least-squares refinement was used for non-hydrogen atoms with anisotropic thermal parameters. Hydrogen atoms except for the P–H hydrogens of all complexes were located by assuming the ideal geometry and were included in the structure calculation without further refinement of the parameters. There are few significant differences in crystallographic data and details of refinement for complexes **1b**, **2b**–**c**, **3a**–**c**, **4a** and **4c** as shown in Table 6. Three methyl carbons (C53–C59 atoms) of the $PH(t\text{-}Bu)_2$ ligand of **2b** were disordered.

5. Supplementary material

CCDC 718321, 718322, 718323, 718324, 718325, 718326, 718327 and 718328 contains the supplementary crystallographic data for **1b**, **2b**, **2c**, **3a**, **3b**, **3c**, **4a** and **4c**. These data can be obtained free of charge from The Cambridge Crystallographic Data Centre via www.ccdc.cam.ac.uk/data_request/cif.

Acknowledgment

This work was financially supported by a Grant-in-Aid for Scientific Research on Priority Areas, from the Ministry of Education, Culture, Sport, Science, and Technology of Japan.

References

[1] J.P. Collman, L.S. Hegedus, J.R. Norton, R.G. Finke, Principle and Applications of Organotransition Metal Chemistry, University Science Books, Mill Valley, CA, 1987.
[2] G.W. Parshall, S. Ittel, Homogeneous Catalysis, Wiley, New York, 1992.
[3] L.H. Pignolet, in: L.H. Pignolet (Ed.), Homogeneous Catalysis with Metal Phosphine Complexes, Plenum, New York, 1983, pp. 1–489.
[4] (a) C.A. Tolman, J. Am. Chem. Soc. 92 (1970) 2953;
(b) C.A. Tolman, J. Am. Chem. Soc. 92 (1970) 2956.
[5] (a) J. Chatt, B.L. Shaw, J. Chem. Soc. (1959) 705;
(b) G.B. Deacon, K.T. Nelson-Reed, J. Organomet. Chem. 322 (1987) 257;
(c) F. Glockling, T. McBride, R.J.I. Pollock, Inorg. Chim. Acta 8 (1974) 77;
(d) F. Glockling, T. McBride, R.J.I. Pollock, Inorg. Chim. Acta 8 (1974) 81;
(e) R.J. Goodfellow, M.J. Hardy, B.F. Taylor, J. Chem. Soc., Dalton Trans. (1973) 2450;
(f) R.J. Goodfellow, M.J. Hardy, B.F. Taylor, J. Chem. Soc., Dalton Trans. (1974) 1676;
(g) J. Ertl, T. Debaerdemaeker, H.A. Brune, Chem. Ber. 115 (1982) 3860;
(h) R. Romeo, G. Alibrandi, Inorg. Chem. 36 (1997) 4822;
(i) V.S. Petrosyan, A.B. Permin, S.G. Sacharov, O.A. Reutov, J. Organomet. Chem. 65 (1974) C7;
(j) P.S. Braterman, R.J. Cross, G.B. Young, J. Chem. Soc., Chem. Commun. (1975) 627;
(k) M. Tanabe, M. Itazaki, O. Kitami, Y. Nishihara, K. Osakada, Bull. Chem. Soc. Jpn. 78 (2005) 1288;
(l) D.T. Clark, D.B. Adams, D. Briggs, J. Chem. Soc., Chem. Commun. (1971) 602;
(m) U. Bayer, H.A. Brune, Z. Naturforsch. B 38b (1983) 226;
(n) C.M. Haar, S.P. Nolan, W.J. Marshall, K.G. Moloy, A. Prock, W.P. Giering, Organometallics 18 (1999) 474.
[6] See for example: K. Osakada, in: R.H. Crabtree, D.M. Mingos (Eds.), Comprehensive Organometallic Chemistry III, vol. 8, Elsevier, Oxford, UK, 2006, pp. 445–609.
[7] (a) Ni complex: M.J. Doyle, J. McMeeking, P. Binger, J. Chem. Soc., Chem. Commun. (1976) 376;
(b) T. Kohara, S. Komiya, T. Yamamoto, A. Yamamoto, Chem. Lett. (1979) 1513;
(c) T. Yamamoto, M. Abla, Y. Murakami, Bull. Chem. Soc. Jpn. 75 (2002) 1997.
[8] Pd complex: F. Ozawa, T. Ito, A. Yamamoto, J. Am. Chem. Soc. 102 (1980) 6457.

[9] (a) Pt complex: M.P. Brown, R.J. Puddephatt, C.E.E. Upton, J. Chem. Soc., Dalton Trans. (1974) 2457;
(b) G.S. Hill, L.M. Rendina, R.J. Puddephatt, Organometallics 14 (1995) 4966;
(c) K.I. Goldberg, J.-Y. Yan, E.M. Breitung, J. Am. Chem. Soc. 117 (1995) 6889;
(d) G.S. Hill, G.P.A. Yap, R.J. Puddephatt, Organometallics 18 (1998) 1408;
(e) D.M. Crumpton, K.I. Goldberg, J. Am. Chem. Soc. 122 (2000) 962;
(f) J.L. Butikofer, J.M. Hoerter, R.G. Peters, D.M. Roddick, Organometallics 23 (2004) 400.
[10] (a) F. Ozawa, T. Ito, Y. Nakamura, A. Yamamoto, Bull. Chem. Soc. Jpn. 54 (1981) 1868;
(b) K. Tatsumi, R. Hoffmann, A. Yamamoto, J.K. Stille, Bull. Chem. Soc. Jpn. 54 (1981) 1857.
[11] (a) P.S. Braterman, R.J. Cross, G.B. Young, J. Chem. Soc., Dalton Trans. (1976) 1310;
(b) P.S. Braterman, R.J. Cross, G.B. Young, J. Chem. Soc., Dalton Trans. (1977) 1892.
[12] S. Shekhar, J.F. Hartwig, J. Am. Chem. Soc. 126 (2004) 13016.
[13] (a) S. Komiya, Y. Morimoto, A. Yamamoto, T. Yamamoto, Organometallics 1 (1982) 1528;
(b) T.M. Miller, A.N. Izumi, Y.-S. Shih, G.M. Whitesides, J. Am. Chem. Soc. 110 (1988) 3146;
(c) T.M. Miller, T.J. McCarthy, G.M. Whitesides, J. Am. Chem. Soc. 110 (1988) 3156;
(d) T.M. Miller, G.M. Whitesides, J. Am. Chem. Soc. 110 (1988) 3164.
[14] (a) I.V. Kourkine, M.B. Chapman, D.S. Glueck, K. Eichele, R.E. Wasylishen, G.P.A. Yap, L.M. Liable-Sands, A.L. Rheingold, Inorg. Chem. 35 (1996) 1478;
(b) D.K. Wicht, I.V. Kourkine, B.M. Lew, J.M. Nthenge, D.S. Glueck, J. Am. Chem. Soc. 119 (1997) 5039;
(c) C. Scriban, I. Kovacik, D.S. Glueck, Organometallics 24 (2005) 4871;
(d) I. Kovacik, C. Scriban, D.S. Glueck, Organometallics 25 (2006) 536;
(e) C. Scriban, D.S. Glueck, J. Am. Chem. Soc. 128 (2006) 2788;
(f) I. Kovacik, D.K. Wicht, N.S. Grewal, D.S. Glueck, Organometallics 19 (2000) 950.
[15] (a) E. Alonso, J.M. Casas, J. Forniés, C. Fortuño, A. Martín, A.G. Orpen, C.A. Tsipis, A.C. Tsipis, Organometallics 20 (2001) 5571;
(b) E. Alonso, J. Forniés, C. Fortuño, A. Martín, A.G. Orpen, Chem. Commun. (1996) 231;
(c) E. Alonso, J. Forniés, C. Fortuño, A. Martín, A.G. Orpen, Organometallics 22 (2003) 2723;
(d) J.M. Casas, J. Forniés, F. Martínez, A.J. Rueda, M. Tomás, A.J. Welch, Inorg. Chem. 38 (1999) 1529;
(e) E. Alonso, J. Forniés, C. Fortuño, M. Tomás, J. Chem. Soc., Dalton Trans. (1995) 3777;
(f) L.R. Falvello, J. Forniés, C. Fortuño, F. Martínez, Inorg. Chem. 33 (1994) 6242;
(g) L.R. Falvello, J. Forniés, C. Fortuño, A. Martín, A.P. Martínez-Sariñena, Organometallics 16 (1997) 5849;
(h) L.R. Falvello, J. Forniés, C. Fortuño, F. Durán, A. Martín, Organometallics 21 (2002) 2226.
[16] M. Itazaki, Y. Nishihara, K. Osakada, Organometallics 23 (2004) 1610.
[17] J. Forniés, C. Fortuño, R. Navarro, F. Martínez, A.J. Welch, J. Organomet. Chem. 394 (1990) 643.
[18] (a) C.R. Kistner, J.H. Hutchinson, J.R. Doyle, J.C. Storlie, Inorg. Chem. 2 (1963) 1255;
(b) H.C. Clark, L.E. Manzer, J. Organomet. Chem. 59 (1973) 411;
(c) H.A. Brune, J. Unsin, H.G. Alt, G. Schmidtberg, K.-H. Spohn, Chem. Ber. 117 (1984) 1606.
[19] I.V. Kourkine, D.S. Glueck, Inorg. Chem. 36 (1997) 5160.
[20] P. Leoni, G. Chiaradonna, M. Pasquali, F. Marchetti, Inorg. Chem. 38 (1999) 253.
[21] P. Mastrorilli, M. Palma, F.P. Fanizzi, C.F. Nobile, J. Chem. Soc., Dalton Trans. (2000) 4276.
[22] J. Forniés, C. Fortuño, S. Ibáñez, A. Martín, Inorg. Chem. 45 (2006) 4850.